Received: 31 July 2020 | Revised: 21 October 2020 | Accepted: 23 October 2020

DOI: 10.1002/jcp.30137

ORIGINAL RESEARCH ARTICLE

Journal of Cellular Physiology WILEY

# Retinoic acid increases phagocytosis of myelin by macrophages

Siyu Wu[1,2] | Lorenzo Romero-Ramírez[1] | Jörg Mey[1,2]

[1]Laboratorio Regeneración Neuronal e Inmunidad Innata, Hospital Nacional de Parapléjicos, Toledo, Spain

[2]School of Mental Health and Neuroscience and EURON Graduate School of Neuroscience, Maastricht University, Maastricht, The Netherlands

**Correspondence**
Jörg Mey, Laboratorio Regeneración Neuronal e Inmunidad Innata, Hospital Nacional de Parapléjicos, SESCAM, Finca la Peraleda s/n, 45071 Toledo, Spain.
Email: jmey@sescam.jccm.es

**Funding information**
Ministerio de Economía y Competitividad, Grant/Award Number: SAF2017-89366R; Chinese Scholarship Coucil, Grant/Award Number: 201606300031

## Abstract

Traumatic injuries of the central nervous system (CNS) are followed by the accumulation of cellular debris including proteins and lipids from myelinated fiber tracts. Insufficient phagocytic clearance of myelin debris influences the pathological process because it induces inflammation and blocks axonal regeneration. We investigated whether ligands of nuclear receptor families retinoic acid receptors (RARs), retinoid X receptors, peroxisome proliferator-activated receptors, lipid X receptors, and farnesoid X receptors increase myelin phagocytosis by murine bone marrow–derived macrophages and Raw264.7 cells. Using in vitro assays with 3,3′-dioctadecyloxacarbocyanine perchlorate- and pHrodo-labeled myelin we found that the transcriptional activator all-*trans* retinoic acid (RA)enhanced endocytosis of myelin involving the induction of tissue transglutaminase-2. The RAR-dependent increase of phagocytosis was not associated with changes in gene expression of receptors FcγR1, FcγR2b, FcγR3, TREM2, DAP12, CR3, or MerTK. The combination of RA and myelin exposure significantly reduced the expression of M1 marker genes inducible nitric oxide synthase and interleukin-1β and increased expression of transmembrane proteins CD36 and ABC-A1, which are involved in lipid transport and metabolism. The present results suggest an additional mechanism for therapeutic applications of RA after CNS trauma. It remains to be studied whether endogenous RA-signaling regulates phagocytosis in vivo.

**KEYWORDS**

bone marrow–derived macrophages, inflammation, myelin phagocytosis, RAR, Raw264.7 cells, retinoic acid, transglutaminase

## 1 | INTRODUCTION

Neurodegenerative pathologies are accompanied by the accumulation of cellular debris, including proteins and lipids from the degradation of myelin (Ek et al., 2012). Following spinal cord injury (SCI), myelin debris constitutes an obstacle for functional regeneration. Three main reasons may account for this: (1) Myelin debris exacerbates the inflammatory response of microglia and macrophages (Kopper & Gensel, 2018). Ingested myelin becomes concentrated in phagocytes, persists there for weeks and contributes to a chronic inflammatory state of the tissue (Greenhalgh & David, 2014). This activation of the innate immune system is largely responsible for the secondary cellular degeneration (Zhou et al., 2019), which causes most of the damage after SCI. (2) One theory to explain the failure of axonal regeneration in the mammalian central nervous system (CNS) is based on the observation that CNS myelin inhibits

axonal growth (McKerracher et al., 1994; Schnell & Schwab, 1990). This is due to the signaling mechanisms triggered by myelin proteins Nogo-A (M. S. Chen et al., 2000), oligodendrocyte myelin glycoprotein, myelin-associated glycoprotein and their receptors on neurons (Barton et al., 2003; Fournier et al., 2002; McKerracher et al., 1994). (3) Extracellular myelin debris arrests the differentiation of oligodendrocyte precursor cells and thereby inhibits the remyelination of axons (Kotter et al., 2006). In the course of its degradation, biochemical alterations of myelin may cause additional autoimmune pathology and demyelination (Caprariello et al., 2018).

A successful recovery process after CNS lesions depends therefore on the clearance of myelin (Grajchen et al., 2018; Neumann et al., 2009). This is accomplished by phagocytosis. The phagocytes in the CNS are activated microglia and, if the blood brain barrier is disrupted, hematogenous macrophages (Brück et al., 1995; Church et al., 2017; Neumann et al., 2009). However, after SCI the endocytosis of myelin proceeds very slowly, such that myelin-associated proteins persist in degenerating fiber tracts for may weeks (Becerra et al., 1995; Buss et al., 2005). This lack of myelin clearance may be related to a deficiency in lysosomal breakdown, as macrophages ingest excessive amounts of cholesterol which is released from disrupted myelin. In multiple sclerosis, a deficient degradation of lipids causes macrophages to adopt an inflammatory phenotype (Grajchen et al., 2018, 2020). Thus, it is clinically important to modulate the uptake and breakdown of myelin by phagocytes without triggering a proinflammatory response.

The present work is based on the hypothesis that nuclear receptors (NRs) which interact with retinoid X receptors (RXRs) can be engaged for this purpose. The RXR are ligand-activated transcription factors that form heterodimeric partners with other NR families, including the lipid X receptors (LXRs), peroxisome proliferator-activated receptors (PPARs), and retinoic acid receptors (RARs; Mey, 2017). This family consists of RARα, RARβ, and RARγ, all of which are endogenously activated by all-*trans* retinoic acid (tRA). Retinoic acid plays a key role in morphogenesis and cellular differentiation of the nervous system. In addition to its function in embryonic development, RA is involved in neurite growth, remyelination, and modulates innate and adaptive immunity (Gonçalves et al., 2018; Huang et al., 2011; Zhelyaznik et al., 2003). A recent review concludes "that RA and its receptors influence the functional fate of just about every immune cell and participate at practically every level and every stage of the immune response" (Larange & Cheroutre, 2016). Retinoids reduce the expression of inducible nitric oxide synthase (iNOS), of proinflammatory cytokines, chemokines, and prostaglandins (Dheen et al., 2005; Gross et al., 1993; Kampmann et al., 2008; van Neerven, Nemes, et al., 2010, van Neerven, Regen, et al., 2010). It has been suggested that the RA signaling pathway constitutes an anti-inflammatory feed-back mechanism in the nervous system (C. Chen et al., 2019; Mey et al., 2007).

The phagocytosis of apoptotic cell bodies by macrophages and microglia is regulated by NRs of the PPAR/RXR, LXR/RXR, and RAR/RXR families. Their activation can increase the expression of phagocytosis receptors on the cell surface (Röszer, 2017). Another key component in endocytosis is the enzyme transglutaminase-2 (TGM2), which is involved in receptor accumulation, formation of the phagocytic cup, and Rho signaling (Nadella et al., 2015; Szondy et al., 2003; Tóth et al., 2009). The expression of TGM2 is regulated by RA (C. Chen et al., 2019; van Neerven, Nemes, et al., 2010). Although the induction of TGM2 was found to increase phagocytosis of apoptotic cells (Rébé et al., 2009) and of myelin (Sestito et al., 2020), it is not known whether RA signaling is involved in regulating the clearance of myelin. The objectives of the present study were therefore (1) to investigate whether activation of RAR/RXR influences myelin clearance, (2) to identify some of the relevant molecular targets of RAR/RXR, and (3) to study how the combined exposure to myelin and retinoids affects the inflammatory phenotype of macrophages.

## 2 | MATERIALS AND METHODS

### 2.1 | Animals

Bone marrow–derived macrophages (BMDM) were isolated from 6-month-old male C57BL/6 mice. For the isolation of myelin debris, we used brains of adult Wistar rats. All animals were bred at the animal facility of the Hospital Nacional de Parapléjicos. Animal care and euthanasia were approved by the Local Ethics Committee on Animal Welfare (163CEEA/2017) in accordance with the European Community Council Directive (86/609/EEC).

### 2.2 | Preparation of BMDM

For the preparation of BMDM, femur and tibia bones of C57BL/6 mice were dissected, thoroughly freed from muscles and connective tissue, sterilized superficially with 70% ethanol and collected in ice cold phosphate-buffered saline (PBS), pH 7.4. Under sterile conditions, bones were cut at both ends below the epiphysis. To extract the bone marrow a 25 or 29-G canula was inserted into the marrow and the bones flushed twice with 2 ml Dulbecco's modified Eagle's medium (DMEM)/10% fetal bovine serum (FBS) from both sides. Extracts from one mouse were collected, spun down (10 min, 1800 rpm) and resuspended in 1 ml lysis buffer, which consisted of 8.29 mg/ml $NH_4Cl$, 1 mg/ml $KHCO_3$, 37 μg/ml EDTA. Following lysis of the erythrocytes for 1 min at room temperature (RT), 14 ml ice cold PBS were added, cells were centrifuged again and the supernatant resuspended in medium. Cells were cultivated in nontreated culture dishes ($d$ = 100 mm) at a density of 10,000,000 cells/plate for 7 days at 37°C, 5% $CO_2$. The macrophage medium consisted of DMEM supplemented with 10% heat inactivated FBS, 1% GlutaMax™ and 1% penicillin/streptomycin (10,000 U/ml), 20 μg/ml murine macrophage-colony stimulating factor (M-CSF; 315-02; Peprotech). After 7 days in culture, adherent cells were approximately 90% pure macrophages, which were used immediately for experiments or stored at −80°C. For detaching BMDM cells from tissue culture plastic, cold PBS was used.

## 2.3 | Myelin isolation and labeling

Myelin was isolated using discontinuous sucrose gradient centrifugation as previously described (Kotter et al., 2006). In brief, adult rat brains were homogenized mechanically in ice-cold 0.32 M sucrose (T25 Digital Ultra-Turrax). The homogenate was laid over a 0.85 M sucrose solution and subjected to ultracentrifugation (75,000*g*, 4°C, 30 min). The interface was recovered and suspended in 20 mM Tris/HCl buffer (12,000*g*, 4°C, 15 min). Pellets were resuspended in this buffer and stored at −80°C until further processing. The protein concentration of the preparation was analyzed with Bio-Rad protein assay, according to the manufacturer's instructions.

Before flow cytometry or immunocytochemistry assays, the required amount of myelin debris was fluorescently labeled using 3,3′-dioctadecyloxacarbocyanine perchlorate (DiO; N22884; Invitrogen). For this, DiO dye was dissolved in dimethyl sulfoxide (DMSO) 1 mg/ml. Myelin was resuspended in PBS, mixed with 1.25% DiO (12.5 μg DiO-DMSO/1 mg myelin), and incubated for 30 min at 37°C. Labeled myelin was spun down and resuspended in PBS and stored at 4°C.

For the analysis of phagocytosis with a microplate reader, myelin was labeled with pHrodo Green STP Ester (Cat. no. P35369; Invitrogen). The pHrodo dye was dissolved in DMSO (500 μg/75 μl DMSO). Myelin extract was resuspended 1/1 (vol/vol) in 0.1 M $NaHCO_3$ (pH 8.4). To this 1% pHrodo-DMSO were added and incubated with for 45 min at RT. The labeled myelin was spun down (8 min, 12,000*g*) and the pellet resuspended (1 mg/ml) in Roswell Park Memorial Institute-1640 (RPMI-1640) medium with 1% FBS. Until use, the labeled myelin suspension was stored at 4°C.

## 2.4 | Cell culture

The murine microglia cell line BV-2 was grown in DMEM/10% FBS supplemented with 1% GlutaMax and 1% penicillin/streptomycin (10,000 U/ml) at 37°C, 5% $CO_2$. When cells had reached confluence, they were detached with trypsin (0.25%), and plated either in 12-well plates at 500,000 cells/well or in 96-well plates at 40,000 cells/well, depending on the assay.

The cell line Raw264.7 of murine macrophages was cultivated in RPMI medium with 5% FBS, GlutaMax and penicillin/streptomycin as indicated above for BV-2 cells. For plating in multiwell dishes, cells were detached from tissue culture plastic with cold PBS. Raw264.7 cells were plated either in 12-well plates at 600,000 cells/well or in 96-well plates at 60,000 cells/well, depending on the assay.

Macrophage primary cultures were grown in the same medium as BV-2 cells with the addition of 20 μg/ml M-CSF (315-02; Peprotech) in 12-well plates at 700,000 cells/well or in 96-well plates at 70,000 cells/well.

## 2.5 | Receptor agonists, antagonists, and enzyme inhibitors

Transcriptional activation of RAR-reporter constructs by tRA was found to be maximal between 0.1 and 10 μM (Allenby et al. 1993), and experiments with glial cultures showed strong effects with 0.01–1 μM (van Neerven, Regen, et al., 2010). To test the molecular regulation of phagocytosis we therefore tested 10 nM, 0.1 μM, and 0.5 μM of the pan-RAR agonist all-tRA (R2625; Sigma); 0.1 and 0.5 μM pan-RXR agonist bexarotene (153559-49-0; LC Laboratories); 1 μM pan-RXR antagonist UVI3003 (3303; Tocris); 1 μM RARβ agonist-RARα/γ antagonist BMS189453 (SML1149; identical to BMS453; Sigma); 1 and 10 μM pan LXR agonist T0901317 (Cay71810-10; Cayman); 9 and 18 μM PPARα agonist fenofibrate (Cay10005368-1; Cayman); 50 nM and 0.1 μM PPARγ antagonist rosiglitazone (LKT-R5773.100; LKT Laboratories); 0.2 and 0.5 μM PPARβ/δ agonist GW501516 (Cay10004272-1; Cayman); 1 and 2 μM FXR agonist GW4064 (Cay10006611-5; Cayman); 0.5 and 1 μM TGM2 inhibitor cystamine dihydrochloride (B22873.14; Alfa Aesar); 15, 25, 50, and 100 μM TGM2 inhibitor ERW1041E (5095220001; Merck); and 1, 5, and 25 μM blocker of scavenger receptor CD36 sulfo-*N*-succinimidyl oleate (SSO; SML2148; Merck).

## 2.6 | Phagocytosis assays

The effect of NRs on endocytosis by BV-2 and Raw264.7 cells was first assessed using SkyBlue beads. Fluorescent latex particles with $d = 0.1–0.3$ μm (FP-0270-2; 1% wt/vol; Spherotch) were suspended 1/1000 in DMEM/5% FBS. Cell cultures in six-well plates were treated with NR agonists for 24 h. Subsequently, 150 μl of SkyeBlue bead suspension were added to the cells. Following 8-h incubation at 37°C, 5% $CO_2$, cells were harvested and the internalization of fluorescent beads quantified with flow cytometry.

In phagocytosis assays with myelin, cells were pretreated for 16 h with agonists and antagonists before the 8 h myelin exposure. We used two independent assays for evaluation with either flow cytometry or a microplate reader. For myelin phagocytosis assays with flow cytometry, cells were incubated with DiO-labeled myelin at 12.5 μg myelin/ml culture medium. Uptake was measured on a FACS Canto machine (BD Biosciences), using identical settings for BV-2 cells or Raw264.7 cells, and analyzed by using FlowJo 7.6 software. The viability marker 7-amino-actinomycin D (1 μg/ml; BD Biosciences) was added 10–15 min before analysis. Phagocytosis was expressed as percentage of live cells that took up myelin and, secondly, as the geometric mean fluorescence intensity of the DiO green fluorescence signal per cell, indicating the total amount of internalized myelin.

For myelin phagocytosis assays with a microplate reader, cells were incubated with 12.5 μg/ml pHrodo-labeled myelin at 37°C for specified periods ranging from 30 min to 72 h. To quantify myelin uptake, we washed cells with PBS to eliminate pHrodo fluorescence

in the cell culture medium. Quantitative assessment of myelin uptake was performed with a fluorescence plate reader (Infinite M1000 Pro; Tecan) using the pHrodo dye excitation and emission maxima of approximately 505 and 525 nm.

## 2.7 | Immunocytochemistry and fluorescence microscopy

After incubation with myelin, cells were washed with PBS, fixed in 4% paraformaldehyde/PBS for 15 min, washed, blocked and permeabilized for 1 h in 10% goat serum, and 0.1% Triton X-100 at RT. Cultures were incubated in blocking buffer with primary antibody against myelin basic protein (MBP; ab7349, 1/2000; Abcam) overnight at 4°C and subsequently with fluorescence-labeled secondary antibody (goat anti-rat, 1/500; A11007; Invitrogen) for 2 h at room temperature. Cell nuclei were stained with Hoechst 33342 (1:2000 in PBS for 2 min) using a Leica Confocal microscope at ×63 magnification and a Leica epifluorescence microscope at ×40 magnification.

## 2.8 | Quantification of gene expression

RNA was isolated with TRIzol (15596018; Invitrogen), according to manufacturer's instructions. To remove genomic DNA, purified RNA was digested with DNase I (EN0521; Thermo Fisher Scientific). An aliquot corresponding to 0.5 μg of purified RNA from BMDM and 2 μg from Raw264.7 cells was used for first-strand complementary DNA (cDNA) synthesis using Superscript III reverse transcriptase and oligo (dT) primers in a final volume of 40 μl (K1632; Invitrogen Life Technologies). This cDNA product was used in subsequent polymerase chain reaction (PCR) reactions. Real-time quantification of genes was performed using a SYBR Green RT-PCR assay. Each 15 μl SYBR green reaction mixture consisted of 1 μl cDNA, 7.5 μl SYBR Green PCR-mix (2X), 0.75 μl forward and reverse primer (10 pM) and 4.75 μl distilled water. PCR was performed with the following cycling conditions: 5 min at 95°C, followed by 40 cycles of 15 s at 95°C, 60 s at 60°C and a separate dissociation step. Specificity of the PCR product was confirmed by examination of the dissociation plots. A distinct single melting peak indicated that only one DNA sequence was amplified during the PCR. The samples were run in triplicates and the level of expression of each gene was compared with the expression of housekeeping gene 60S ribosomal protein L4 (RPL4). Amplification, detection of specific gene products and quantitative analysis were performed using an ABI 7500 sequence detection system (Applied Biosystems). Three or four independent cell culture preparations were analyzed in all experiments. PCR efficiency was verified by dilution series (1, 1/3, 1/9, 1/27, 1/81, and 1/243) and relative messenger RNA (mRNA) levels were calculated using the comparative $\Delta C_t$ method with normalization to the housekeeping gene. The gene identifiers, primer sequences, product sizes, and melting temperatures are listed in Table 1.

## 2.9 | Western blot analysis

Proteins from Raw264.7 cells and BMDM were extracted with lysis buffer (containing 1% NP-40; 0.2% sodium dodecyl sulfate [SDS]; 0.5 mM dithiothreitol; 20 mM Tris-buffered saline [TBS]) containing protease inhibitor (04693124001; Roche) and phosphatase inhibitor cocktails (04906845001; Roche). Protein concentration was determined with Bio-Rad protein assay (Cat. no. 5000001, based on the Bradford method). For the analysis, 25 μg extract was boiled in loading buffer for 10 min and separated by 8% standard SDS–polyacrylamide gel electrophoresis and wet-transferred to nitrocellulose membranes (Mini-PROTEAN Tetra Cell System; Bio-Rad). Membranes were washed with Tris-buffered saline containing 0.1% Tween20 (TBS-T) and blocked with 5% bovine serum albumin (BSA; A9647; Sigma) in TBS-T. Primary antibodies for TGM2 (rabbit polyclonal, 3557, 1:2500; Cell Signaling), CD36 (mouse monoclonal, sc-7309, 1:800; Santa Cruz), anti glyceraldehyde phosphate dehydrogenase (GAPDH, mouse monoclonal, mab374, 1:500; Millipore) and α-actinin (mouse monoclonal, 612576, 1:5000; BD Pharmingen) were used to incubate the membranes at 4°C overnight. Detection was with appropriate peroxidase-conjugated secondary antibodies (goat anti-rabbit IgG, goat anti-mouse IgG, 111-035-003, 115-035-003; Jackson ImmunoResearch), which were developed with Clarity Western ECL substrate (RPN2232; GE Healthcare) and documented using an Amersham Imager 600. Densitometric analysis was performed using FlowJo 7.6 software. Integrated density data of IR bands were normalized to IR of nonregulated proteins with GAPDH as a loading control for CD36 and α-actinin for TGM2.

## 2.10 | Statistical analysis

Data are presented as mean values ± *SEM*. Nonparametric data are represented as box and whiskers graphs (median, 25/75 percentile, range). Effects of different treatment conditions were analyzed with one-factor analysis of variance using GraphPad Prism v5 software. In case of significant effects, treatment conditions were compared with post hoc Dunnett's or Tukey tests depending on the question. In some cases, when data were normalized to the control condition, we used used one-sample *t*-tests considering $p < .05$ as statistically significant.

# 3 | RESULTS

## 3.1 | RA modulates phagocytosis activity by microglia and macrophage cell lines

To test whether NR agonists influence the activity of phagocytes, we first assessed the uptake of fluorescent latex particles (Skyblue beads), which were not expected to activate specific receptors or induce an inflammatory phenotype. Macrophages of the BV2 cell line were placed in low-serum medium and treated with tRA for 12 h. Subsequently, latex beads were added for an additional incubation

**TABLE 1** Gene indentifiers and primer sequences used in quantitative real-time-polymerase chain reaction

| Gene | Gene ID (NCBI) | Primer sequences | Product $T_m$ (°C) | Product size (bp) |
|---|---|---|---|---|
| RPL4 | NM_024212 | Sense: AGATGATGAACACCGACCTTAGC<br>Antisense: CGGAGGGTCCTTTGGATTTC | 60 | 61 |
| FcγR1 | NM_010186 | Sense: AGG TTCCTCAATGCCAAGTG<br>Antisense: ATTCTTCCATCCGTGACACC | 58 | 127 |
| FcγR2b | NM_001077189 | Sense: CTAGGAAGGACACTGCACCA<br>Antisense: GACAGCAATCCCAGTGACAG | 59 | 114 |
| FcγR3 | NM_001356511 | Sense: TTTGGACACCCAGATGTTTCA<br>Antisense: GTCTTCCTTGAGCACCTGGAT | 60 | 163 |
| TREM2 | NM_001272078 | Sense: CTGGAACCGTCACCATCACTC<br>Antisense: CGAAACTCGATGACTCCTCGG | 62 | 183 |
| DAP12 | NM_011662 | Sense: GCTCTGGAGCCCTCCTGGTGC<br>Antisense: CTCAGTCTCAGCAATGTGTTG | 62 | 261 |
| CR3 | NM_008401 | Sense: GACCCTGGCCGCTCACGTATC<br>Antisense: TCCACGCAGTCCGGTAAAATT | 62 | 127 |
| CD36 | NM_001159557 | Sense: GGAGCCATCTTTGAGCCTTCA<br>Antisense:GAACCAAACTGAGGAATGGATCT | 61 | 217 |
| TGM2 | NM_009373 | Sense: GACAATGTGGAGGAGGGATCT<br>Antisense: CTCTAGGCTGAGACGGTACAG | 60 | 120 |
| MerTk | NM_008587 | Sense: CAGGGCCTTTACCAGGGAGA<br>Antisense: TGTGTGCTGGATGTGATCTTC | 61 | 111 |
| RARα | NM_001177303 | Sense: TTCTTTCCCCCTATGCTGGGT<br>Antisense: GGGAGGGCTGGGTACTATCTC | 62 | 150 |
| RARβ | NM_011243 | Sense: GATGACACAGAAACAGGC<br>Antisense: CTTGAACTTGGGGTCAAG | 60 | 320 |
| RARγ | NM_011244 | Sense: CTGGAGATGGATGACACC<br>Antisense: GTTCTCCAGCATCTCTCG | 60 | 294 |
| IL1β | NM_008361 | Sense: CTGGTGTGACGTTCCCATTA<br>Antisense: CCGACAGCACGAGGCTTT | 57 | 74 |
| iNOS | NM_010927 | Sense: ACATTGATCTCCGTGACAGCC<br>Antisense: CCCTTCAATGGTTGGTACATG | 60 | 158 |
| IL10 | NM_010548 | Sense: GATGCCCCAGGCAGAGAA<br>Antisense: CCCAGGGAATTCAAATGCT | 57 | 57 |
| Arg1 | NM_007482 | Sense: GAACACGGCAGTGGCTTTAAC<br>Antisense: TGCTTAGCTCTGTCTGCTTTG | 59 | 155 |
| ABCA1 | NM_013454 | Sense: TTGGATGGATTAGATTGGAC<br>Antisense: ATGCCTGTGAACACGATG | 60 | 266 |

*Note*: All gene sequences are from mouse.

period of 4 h (Figure 1a), and their uptake was assessed with flow cytometry. Under control conditions, 48.7% of the BV-2 cells showed endocytotic uptake of at least one particle. Treatment with 0.1 μM RA increased this to 57.3% (Figure 1b–e).

To confirm the involvement of the permissive NR RXR in the effect of RA on endocytosis, we preincubated cells with the competitive RXR receptor antagonist UVI3003, with the RXR agonist bexarotene, or a combination of these. As observed for RA, incubation with bexarotene resulted in a significant increase in endocytosis. Cotreating cells with 0.1 μM UVI3003 and RA simultaneously blocked the increase of bead uptake, indicating that the effect of RA depended on NR binding (Figure 1f). Similar experiments were then carried out in the macrophage cell line Raw264.7. Under the same conditions these cells showed a higher level of phagocytic ingestion of SkyeBlue beads than the BV-2 cells, which could not be increased further pharmacologically (Figure 1g).

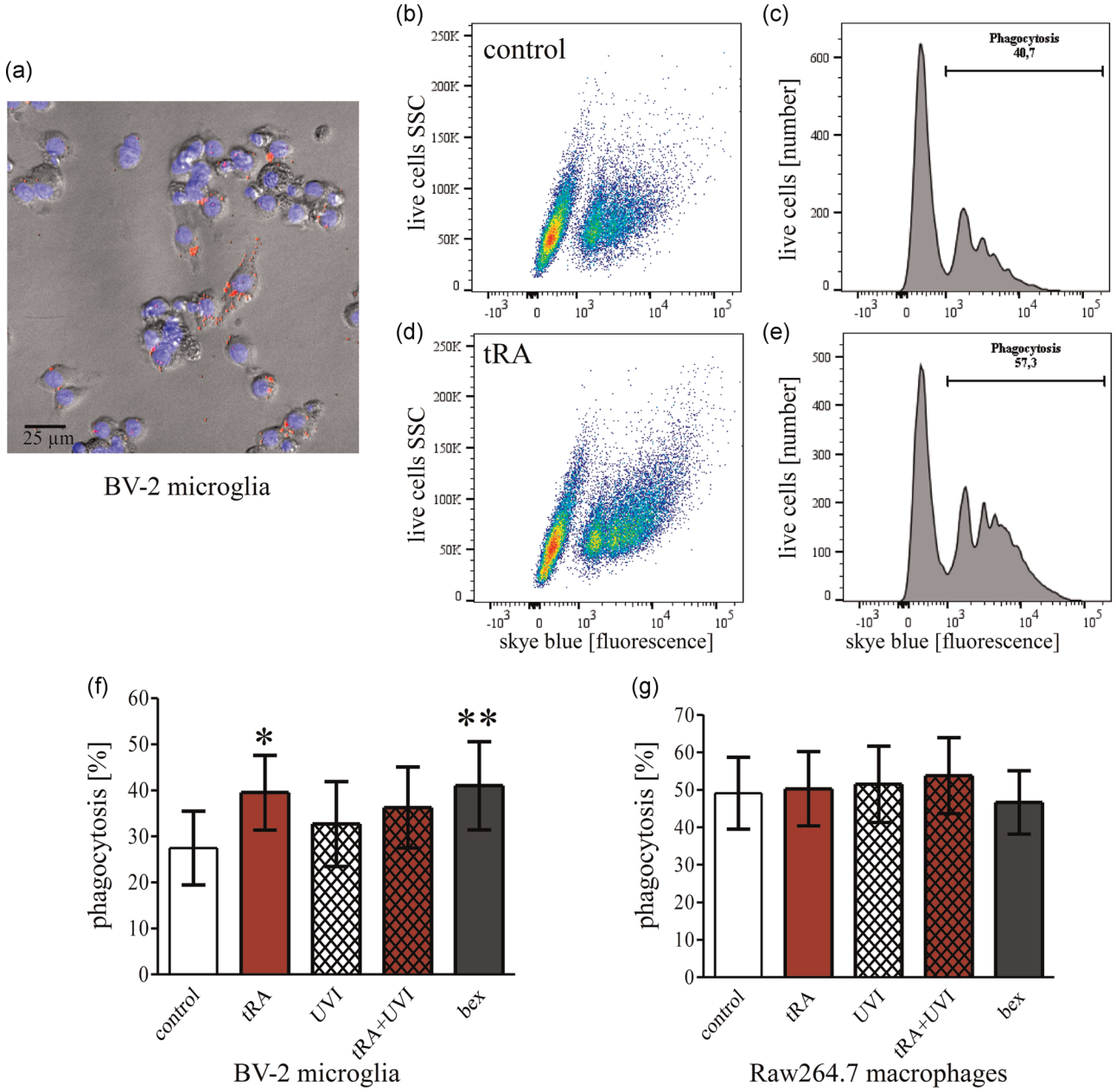


**FIGURE 1** Retinoic acid receptor and retinoid X receptors agonists increase phagocytosis of SkyeBlue beads by BV-2 cells. (a) Phase-contrast image illustrating endocytosis of latex beads (red) by BV-2 cells; nuclei are labeled with Hoechst 33342 (blue). (b–e) Evaluation of endocytosis with flow cytometry showing plots of side scatter/skyblue bead fluorescence in live cells (7-amino-actinomycin D exclusion) (b, d) and cell counts/fluorescence level (c, e). Note distinct peaks indicating the absence or presence of one, two, or more intracellular latex beads. Examples show BV-2 cultures without treatment (b, c) and after 12 h treatment with all-*trans*retinoic acid (tRA) (d, e), followed by 8 h incubation with latex particles. (f–g) Quantification of endocytosis of SkyeBlue beads phagocytosis by BV-2 (f) and Raw264.7 cells (g). Treatment conditions indicate 0.1 μM tRA, 10 nM UVI3003 (UVI), 0.1 μM bexarotene (Bex) or a combination of these; the level of phagocytosis is indicated by the percentage of live cells with at least one internalized SkyBlue bead; bars show mean and*SEM*of five independent experiments;*t*-tests, $^{*}p < .05$; $^{**}p < .01$ (statistical comparison with nontreated controls)

## 3.2 | Effect of NR/RXR agonists on myelin phagocytosis by macrophages

While the ingestion of latex beads gives an indication of general endocytosis activity, the uptake of CNS myelin is physiologically more relevant and may be be regulated differently. To investigate pharmacological effects on myelin clearance, we established a cell culture assay using Raw264.7 macrophages, which were exposed to myelin purified from rat brains and labeled with DiO. Following 12 h pharmacological treatment, cells were incubated for 8 h with fluorescent myelin debris. To validate the assessment of myelin phagocytosis based on the cytometric detection of DiO, the intracellular

uptake of DiO-fluorescent myelin was visualized with confocal microscopy (Figure 2a,b). In addition, staining experiments were carried out using an antibody against MBP. Whereas Raw264.7 macrophages showed no MBP immune reactivity, following treatment with DiO-labeled myelin, intracellular MBP was detected in most cells, and this increased after treatment with all-tRA (Figure 2c–e).

Based on the evidence derived from fluorescence microscopy, we decided to quantify myelin phagocytosis with flow cytometry (Figure 3). Treatment with all-tRA caused a statistically significant increase in the percentage of Raw264.7 cells that had taken up myelin (control: 29.5%, all-tRA: 37.9%). This was similarly observed in bexarotene treated cultures (Figure 3d), indicating that RXR activation alone might increase phagocytosis.

This was compared to the effect of agonists that activate other NRs which also form heterodimers with RXR. To carry out more experiments in parallel, a different assay was established based on pHrodo labeling of myelin (Figure 4a). This dye is characterized by a pH dependent fluorescence, such that fluorescence measurements in a microplate reader reflect accumulation of myelin-pHrodo within acidic lysosomes of the phagocytes. After Raw264.7 cells had been incubated with NR agonists for 12 h, we added pHrodo-labeled myelin and then monitored the pHrodo signal over the course of 24 h. The plot (Figure 4b) shows results of 10 experiments (one per incubation period) with duplicate samples that were measured for total integrated intensity of the pHrodo signal. The background fluorescence in the absence of myelin did not increase over time. As indicated by pHrodo fluorescence, myelin ingestion rose steadily during the first 6 h and was stronger after treatment with all-tRA. This effect was largest between 8- and 12-h incubation.

Based on this result we chose 8 h exposure to pHrodo-myelin and pretreated the cells with the following drugs: All-tRA (panRAR agonist), BMS189453 (RARβ agonist and RARα/γ antagonist), bexarotene (panRXR agonist), fenofibrate (PPARα agonist), GW501516 (PPARβ/δ agonist), rosiglitazone (PPARγ agonist), T0901317 (LXRα/β agonist), and GW4064 (FXR agonist). RA and bexarotene (Figure 4c) significantly increased myelin phagocytosis (Figure 4c), but none of the other NR agonists did (Figure 4d). When activation of RARα and RARγ was blocked with BMS189453, RA still had the same effect on phagocytosis, indicating involvement of the receptor RARβ. All three RAR were expressed by the cells, and the gene expression of RARβ, which is a known transcriptional target of RA itself, significantly increased after RA treatment (data not shown).

To confirm that the observed effects of RA on myelin phagocytosis in Raw264.7 cells extends to primary macrophages, BMDM were purified from adult mice. Cells were treated with RA for 12 h and subsequently exposed to pHrodo-labeled myelin for 1, 2, and 8 h.

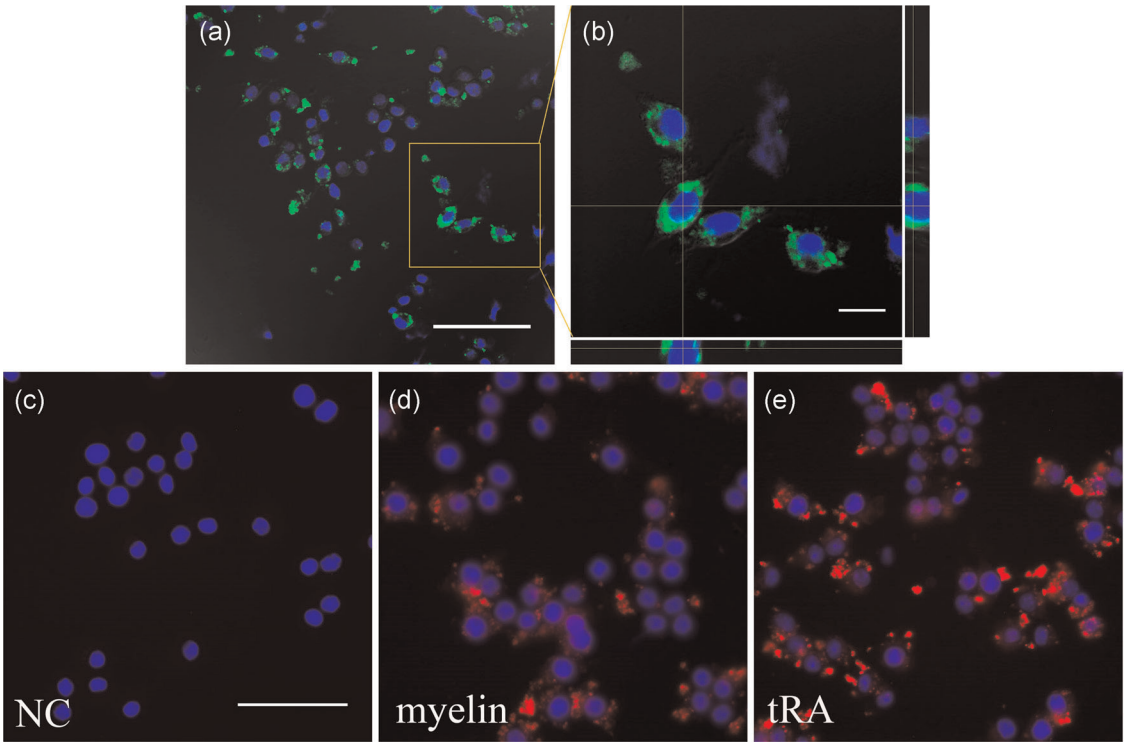


**FIGURE 2** Myelin phagocytosis by Raw264.7 cells. (a, b) Localization of 3,3′-dioctadecyloxacarbocyanine perchlorate-labeled myelin (green fluorescence) within Raw264.7 cells as visualized by confocal laser scanning microscopy. Nuclei are labeled with Hoechst 33342 (blue). Cells with and without internalized myelin are shown at higher magnification (b, confocalZstack image). (c–e) Myelin debris is visualized using anti-myelin basic protein immunocytochemistry (red). Photographs show Raw264.7 cells, whose nuclei are labeled with Hoechst 33342 in cultures without myelin (c), after 8-h incubation with myelin debris (d) and after 12-h treatment with 0.1 μM all-*trans*retinoic acid (tRA) followed by 8-h incubation with myelin debris (e). Scale bars represent (a, c–e) 50 or (b) 10 μm

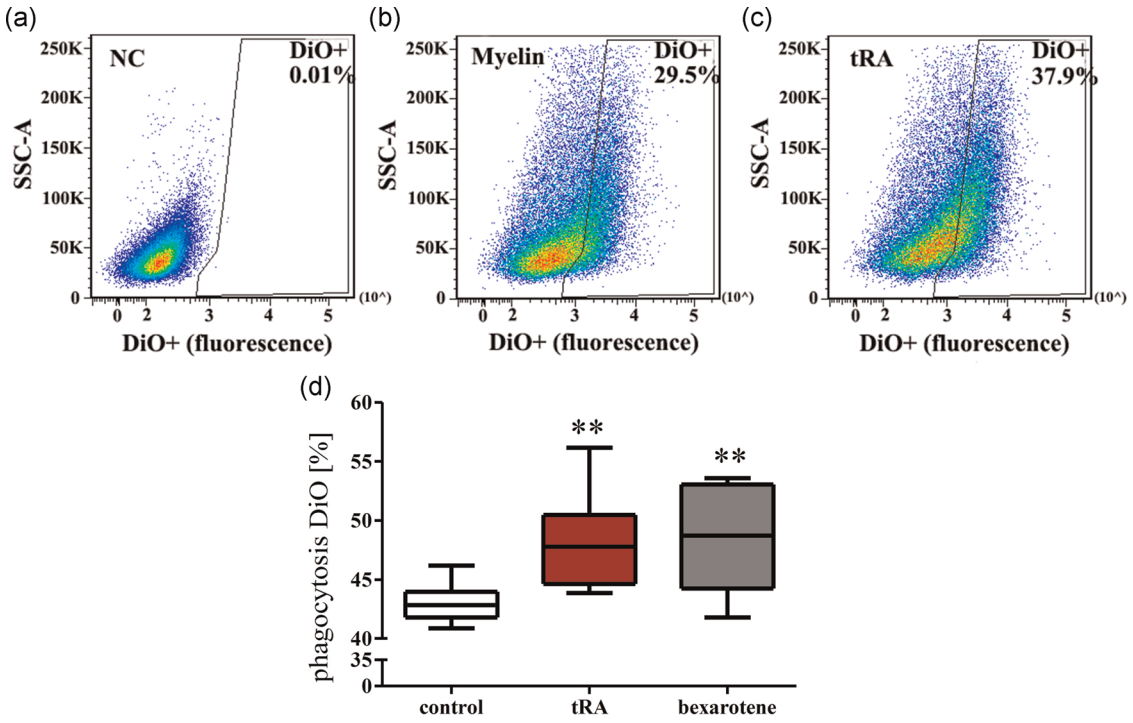


**FIGURE 3** Treatment with all-*trans*retinoic acid (tRA) enhances phagocytosis of 3,3′-dioctadecyloxacarbocyanine perchlorate (DiO)-labeled myelin in Raw264.7 cells. (a–c) DiO-labeled myelin was used to measure endocytosis of myelin debris by flow cytometry. Only live cells were evaluated, based on exclusion of 7-amino-actinomycin D. Plots show counts of Raw264.7 cells without myelin (a); incubated with myelin (b) and after 12-h treatment with 0.1 μM all-tRA followed by 8-h incubation with myelin debris (c). (d) Quantification of the effect of retinoic acid receptor/retinoid X receptor agonists on myelin uptake by Raw264.7. Treatment with RA raised the percentage of DiO/myelin-positive live cells from 43% to 47%, and treatment with bexarotene to 48%. Box and whiskers plots show medians, 25/75 percentiles and ranges; Kruskal–Wallis*H*-test, $p < .001$, was followed by post hoc comparison with nontreated controls $^{**}p < .01$

To ascertain the validity of the procedure, pHrodo-labeled myelin inside the BMDM cells was also stained with MBP immunocytochemistry and documented with confocal microscopy (Figure 5a–c). In BMDM cells, myelin ingestion was observed earlier (already 1 h after treatment) than in Raw264.7 cells. Similarly to the macrophage cell line, BMDM also showed a significant increase of myelin phagocytosis in response to RA and bexarotene (Figure 5d).

## 3.3 | Treatment of macrophages with all-tRA affects gene expression of the scavenger receptor CD36 and enzyme TGM2

To investigate possible mechanisms involved in the effect on phagocytosis, we tested whether the transcriptional activator RA affected the gene expression of surface receptors that are potentially involved in the process (Figure 6). When myelin is opsonized with IgGs or the complement system, endocytosis can be triggered by Fcγ-receptors (FcγR) or complement receptor-3 (CR3). Nonopsonized lipids are recognized by the scavenger receptor CD36. In addition to these, we measured expression of triggering receptor expressed on myeloid cells 2 (TREM2) and its adapter protein DAP12, which have been implicated in phagocytosis of β-amyloid and apoptotic cells. The expression of two enzymes, tissue TGM2 and tyrosine kinase MerTK, were measured to test whether effects or RA were related to alterations of intracellular signaling triggered by myelin-activated receptors. Previous investigations indicated that TGM2 is involved in clustering of phagocytosis receptors (Nadella et al., 2015, Szondy et al., 2003) and that its expression is regulated by RA (van Neerven, Regen, et al., 2010).

All of these genes were found to be expressed in Raw264.7 cells and BMDM, and their basal expression patterns were similar in both types of macrophages, when compared to transcript concentrations of the housekeeping gene RPL4 (Figure 6a,b, note logarithmic scale). By far the highest relative mRNA levels were observed for TREM2 and DAP12. Receptors FcγR3 and CD36 and the enzyme TGM2 were more strongly expressed in BMDM than in Raw264.7 cells. The other receptors had intermediate expression levels of in both types of macrophages. RA treatment in combination with myelin exposure caused an upregulation of the scavenger receptor CD36 in BMDM (Figure 6f) but not in Raw264.7 macrophages. None of the other phagocytosis receptors genes were significantly increased after treatment, and CR3 expression was even reduced in the cell line (Figure 6c–f). Unexpectedly, RA treatment was associated with a decrease in TREM2 mRNA in Raw264.7 cells.

By far the strongest change occurred in the gene expression of TGM2. The cell line showed a 10-fold increase of TGM2 transcripts

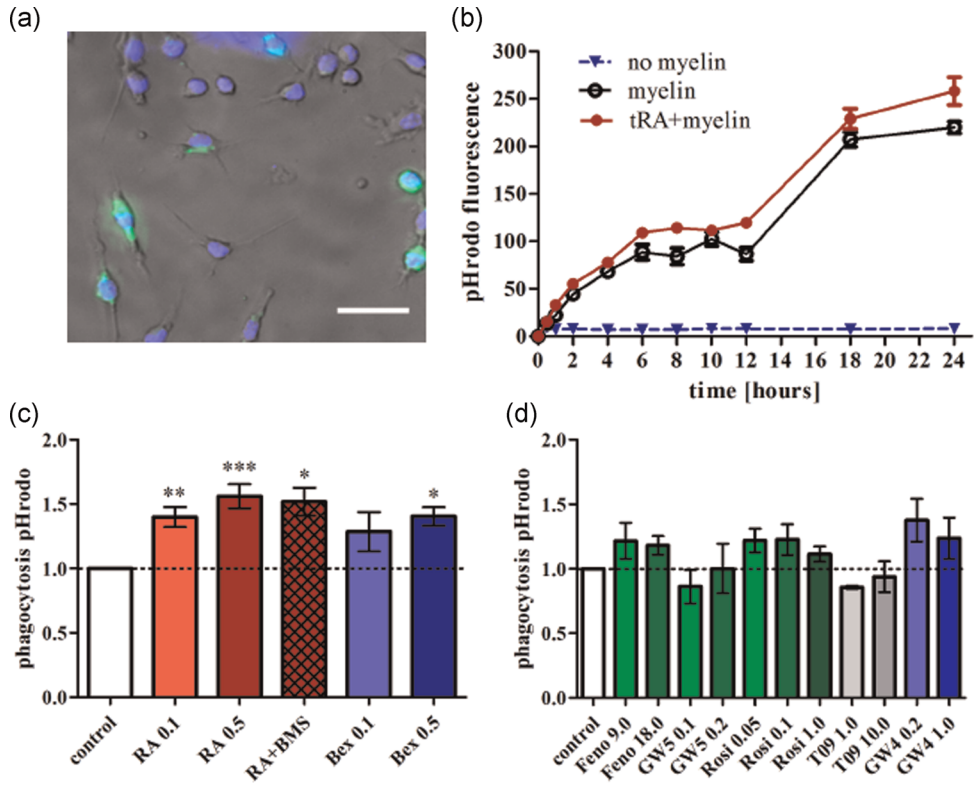


**FIGURE 4** Effect of nuclear receptor (NR) agonists on phagocytosis of pHrodo-labeled myelin by Raw264.7 cells. (a) Phase-contrast image illustrating endocytosis of pHrodo-labeled myelin (superimposed green fluorescence) by Raw264.7 cells; nuclei are labeled with Hoechst 33342 (blue fluorescence), scale bar = 30 µm. (b) Fluorescence intensity of pHrodo-labeled myelin was measured with a microplate reader for 24 h (independent cultures for each time interval). Cells were pretreated with 0.5 µM retinoic acid (RA) for 12 h. (c) Quantification of the effect of nuclear receptor agonists on myelin phagocytosis; treatment conditions indicate incubation with 0.1 and 0.5 µM all-*trans*RA, 0.5 µM all-*trans*RA + 1 µM BMS189453 (tRA + BMS), 0.1 and 0.5 µM bexarotene (Bex). The pHrodo fluorescence intensities were normalized to control (myelin, no NR agonist); bars show means ± *SEM* of five independent experiments; one-way analysis of variance (ANOVA; $F = 4.8$, $df = 5$, $p < .001$) was followed by post hoc Dunnett's comparison with nontreated controls; $^{*}p < .05$, $^{**}p < .01$, $^{***}p < .001$. (d) Treatment conditions indicate incubation with 1 and 10 µM T0901317, 9 and 18 µM fenofibrate, 0.1 and 0.2 µM GW501516 (GW5), 0.2 and 1 µM GW4064 (GW4); quantification as in Panel c; one-way ANOVA ($F = 1.3$, $df = 11$, $p = .2$) showed no significant differences between groups

after RA treatment. This was augmented in the presence of myelin (>35-fold; Figure 6e; $p < .001$). The latter effect was also observed in BMDM (Figure 6f; $p < .05$), although RA or myelin alone did not cause a significant increase in the expression of this enzyme in the primary cultures. Messenger levels of MerTK were not significantly affected by treatment (data not shown).

On the protein level, both cell types contained high amounts of CD36, but no significant increase was found after treatment except for the combination of RA and myelin (Western blot analysis; Figure 7a,b). Under control conditions as well as in the presence of myelin, there was no immunoreactivity of TGM2 in Raw264.7 cells. In accordance with data on gene transcription, incubation with RA induced the production of TGM2 protein (Figure 7c). Additional exposure to myelin increased this further, though not quite significantly ($0.05 < p < .1$). In contrast to the Raw264.7 cell line, BMDM produced TGM2 protein even under control conditions. The increase after RA treatment and myelin exposure was smaller. It reached statistical significance when RA treatment was combined with the addition of myelin to the cells (Figure 7d).

### 3.4 | The modulation of myelin phagocytosis by RA involves CD36 and TGM2

To test whether the effect of RA on phagocytosis is dependent on CD36 or TGM2, we performed pHrodo phagocytosis experiments as described before using specific inhibitors. The scavenger receptor was blocked with 25 µM SSO (Grajchen et al., 2020). The activity of TGM2 was inhibited with 0.5 µM cystamine (Eligini et al., 2016) or 50 µM ERW1041E (Chrobok et al., 2018). Again, RA treatment significantly increased the endocytosis of myelin (Figure 8). In Raw264.7 macrophages this effect was completely abolished with the addition of the CD36 inhibitor SSO ($p < .05$). Cystamine reduced the RA-dependent increase of myelin phagocytosis by half, though this just fell short of the required level of significance ($0.05 < p < .1$). In BMDM, we observed a similar tendency, that is, increased myelin phagocytosis after RA treatment and the inhibition of this effects when CD36 or TGM2 activity were blocked. Application of CD36 or TGM2 inhibitors in the absence of RA did not significantly reduce or increase phagocytosis (data not shown).

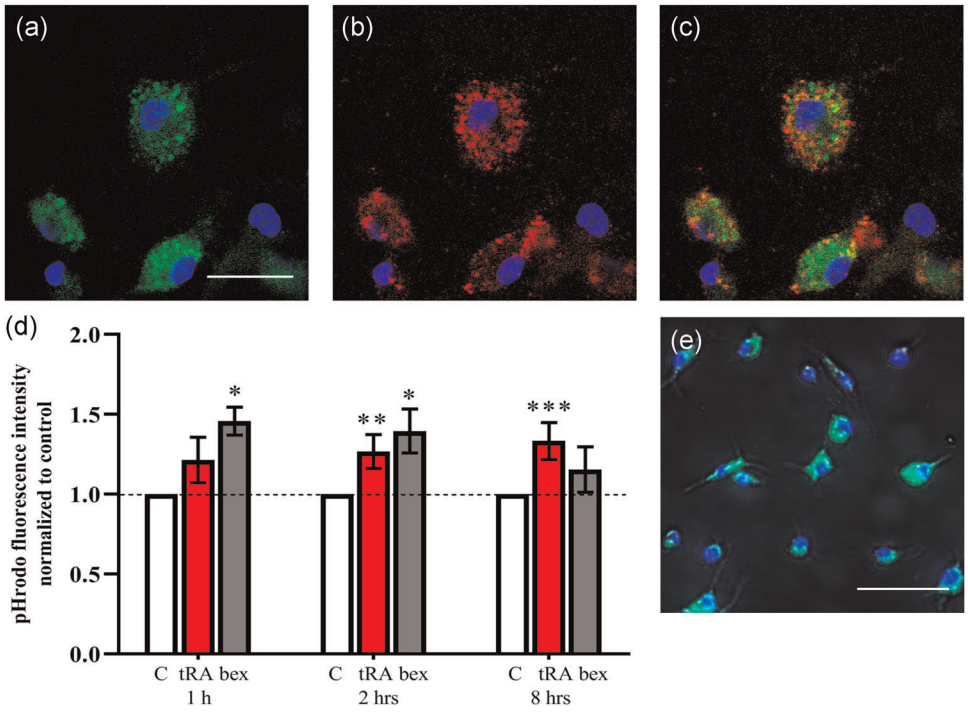


**FIGURE 5** Treatment with retinoic acid (RA) enhanced myelin phagocytosis in bone marrow–derived macrophages (BMDM). (a–c) Colocalization of 3,3′-dioctadecyloxacarbocyanine perchlorate-labeled myelin (green) and myelin basic protein immunocytochemical staining (red) in BMDM. Nuclei are labeled with Hoechst 33342 (blue). (d) Quantification of myelin phagocytosis by BMDM. Cells were treated 12 h with vehicle, 0.1 μM all-*trans*RA (tRA) or 0.1 μM bexarotene followed by 1, 2, and 8 h incubation with myelin debris. Bars show mean and*SEM*of four independent experiments; $^{*}p < .05$, $^{**}p < .01$, $^{***}p < .001$ (in comparison with nontreated controls). (e) Phase-contrast image illustrating endocytosis of pHrodo-labeled myelin (green) by BMDM; nuclei are labeled with Hoechst 33342 (blue). Scale bars represent 20 (a–c) and 50 μm (e). The same experiments were carried out with 0.5 μM RA with similar results

### 3.5 | Interaction between myelin phagocytosis and the inflammatory phenotype of macrophages?

The relation between phagocytosis activity and the inflammatory phenotype of macrophages is influenced by additional environmental factors acting upon the cells. We investigated whether the exposure of CNS myelin affected the expression of genes that are considered hallmarks of a pro- or anti-inflammatory phenotype. These were the iNOS, interleukin-1β (IL-1β), IL-10, and arginase-1 (Arg-1). Additionally, expression of the ATP-binding cassette transporter-A1 (ABC-A1) was studied because this is an important regulator of cholesterol and phospholipid efflux that affects phagocytosis related signaling pathways (Morizawa et al., 2017).

Using the macrophage cell line, we found no significant influence of myelin per se on any of the regulators mentioned above. However, all-tRA significantly reduced the expression of iNOS and IL-1β (Figure 9a,b), confirming earlier studies (van Neerven, Nemes, et al., 2010). There was no influence of myelin or RA with respect to the anti-inflammatory markers IL-10 and Arg-1 (Figure 9c,d). Interestingly and in accordance with its positive effect on myelin endocytosis, RA caused a strong and highly significant upregulation of ABC-A1 (Figure 9e). The Raw264.7 cells expressed all three known RA receptors, RARα, RARβ, RARγ. Of these, RARβ, which is a known transcriptional target of RA, was upregulated after RA treatment (data not shown), suggesting that this NR may be involved in the regulatory effects of RA. However, when using BMS189453, which activates RARβ signaling while blocking RARα and RARγ, the inhibitory effects of all-tRA on iNOS and IL-1β transcription as well as the positive effects on ABC-A1 transcription were abrogated.

## 4 | DISCUSSION

The clearance of myelin debris or the lack thereof are important factors for the outcome of neurodegenerative pathologies. The present experiments demonstrate that the transcriptional activator tRA enhances the ability of macrophages, specifically murine BMDM and Raw264.7 cells to phagocytose myelin. This response, which involves the ligand-activated transcription factor RARβ, could also be elicited with bexarotene, a pharmacological agonist of RXRs, but not with agonists of related NRs PPARα, PPARβ/δ, PPARγ, LXR, or FXR. RARs are generally not considered to need ligand bound RXR and would not be permissive in the absence of an RAR ligand (Mey, 2017; Röszer, 2017). As a possible exception to this model, the present experiments show an effect of the RXR ligand bexarotene alone. The inhibitory effect of the RXR antagonist UVI2002 indicates the requirements of RAR/RXR heterodimers in the process. The RA-dependent mechanism involves the enzyme TGM2. Its transcript and

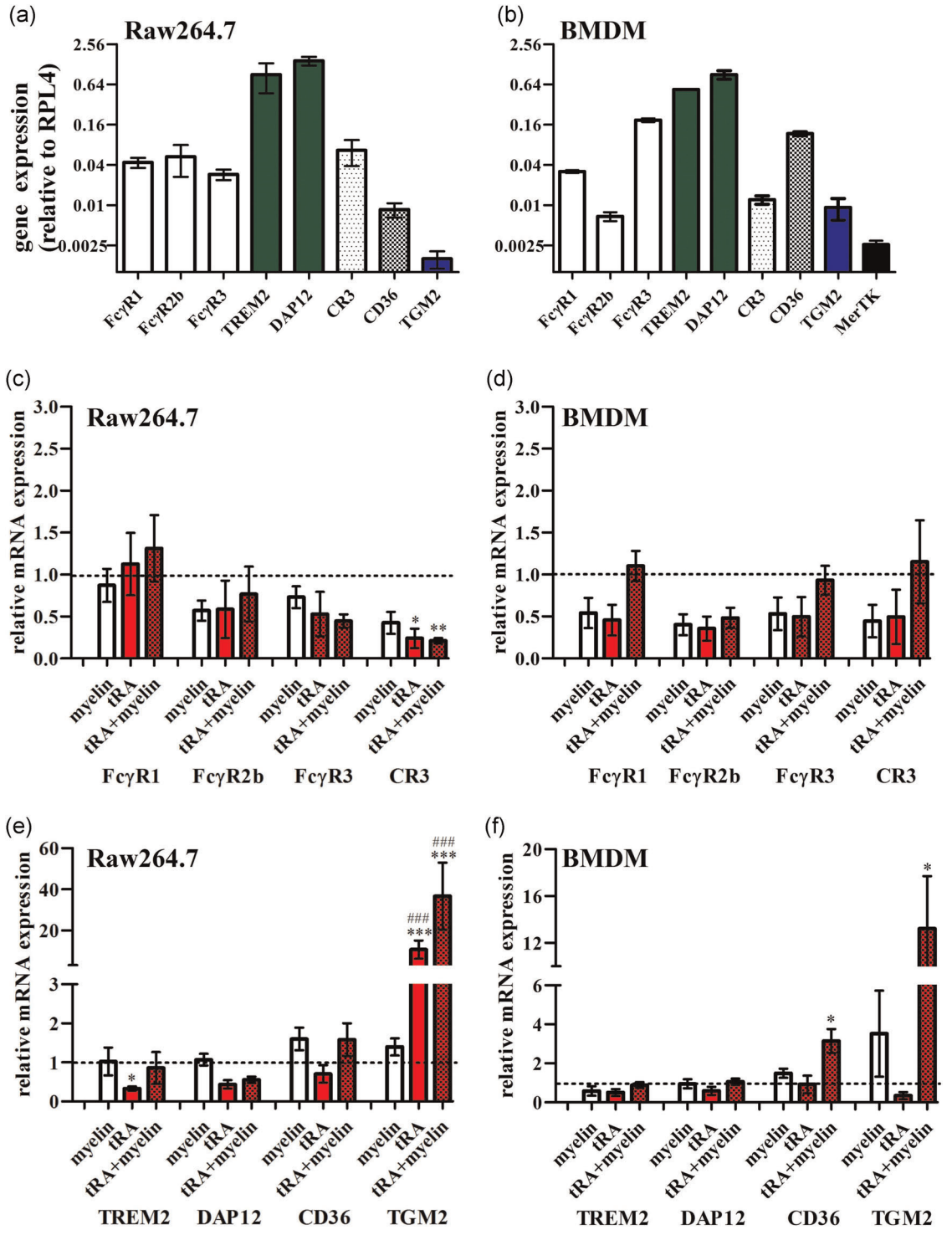


**FIGURE 6** Effect of myelin exposure and RA treatment on the expression of phagocytosis receptor genes. (a, b) Basal gene expression of FcγR1, FcγR2b, FcγR3, TREM2, adapter protein DAP12, CR3, CD36, enzymes TGM2 and MerTK in Raw264.7 cells (a) and bone marrow–derived macrophages (BMDM) (b); messenger (mRNA) levels are expressed relative to the housekeeping gene RPL4. (c–f) Changes of mRNA expression of these genes following 8-h exposure to myelin, 12-h treatment with all-*trans*RA or both; expression levels in Raw264.7 cells (c, e) and BMDM (d, f) are normalized to the control condition without myelin as shown in a and b. Results are from$n$ = 3–4 independent experiments, each measured in triplicates (analysis of variance [ANOVA] is statistically significant for Raw264.7-CR3 [$df$ = 3, 12; $F$ = 5.2; $p$ < .05], Raw264.7-TGM2 [$df$ = 3, 12; $F$ = 4.0; $p$ < .05], BMDM-CD36 [$df$ = 3, 8; $F$ = 8.1; $p$ < .01], BMDM-TGM2 [$df$ = 3, 8; $F$ = 6.5; $p$ < .05] and not significant in all other cases; results of post-hoc Tukey tests as indicated in the graphs: $^{*}p$ < .05, $^{**}p$ < .01, $^{***}p$ < .001 compared to control without myelin, $^{\#\#\#}p$ < .001 compared to myelin treatment)

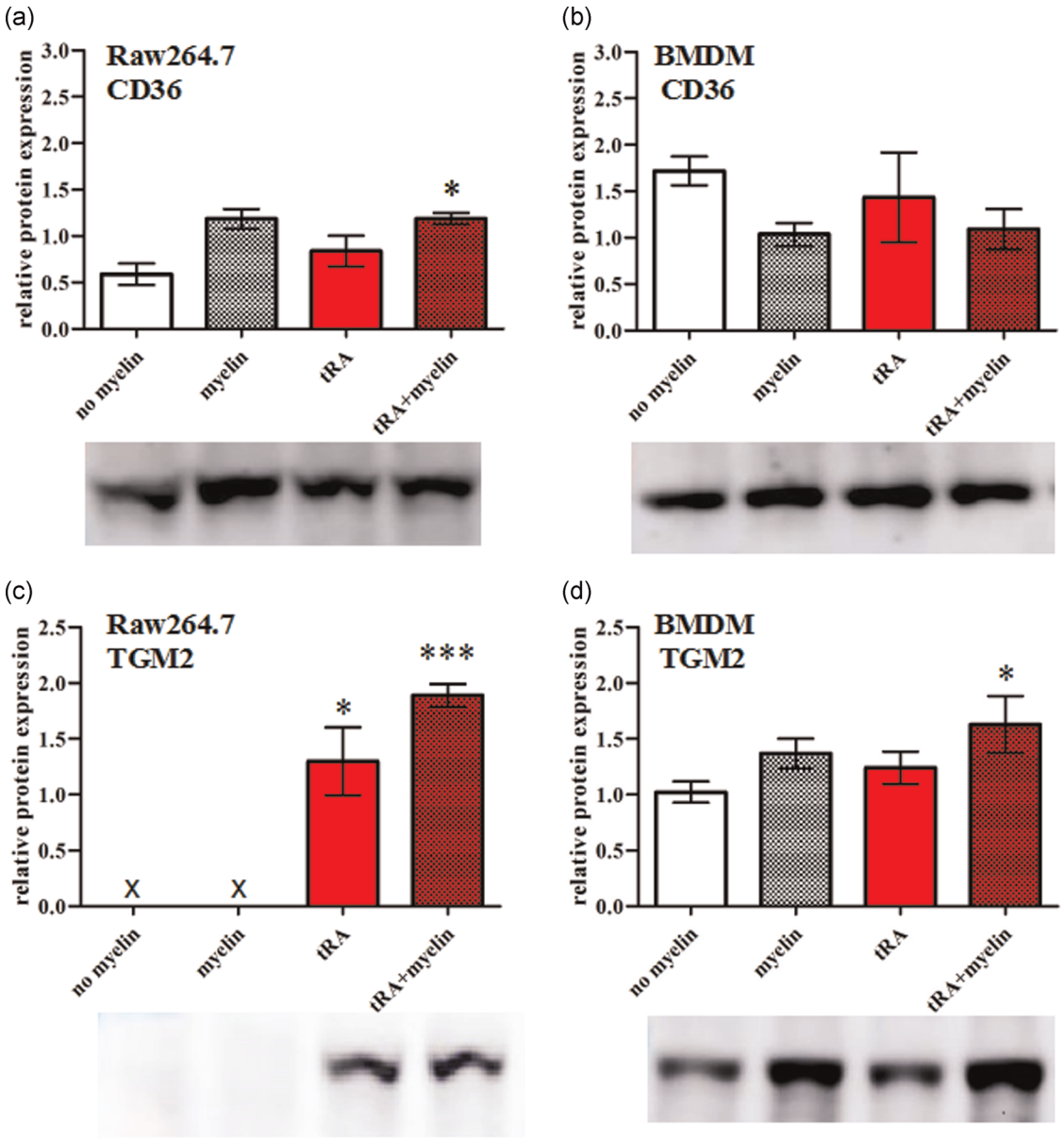


**FIGURE 7** Effect of retinoic acid (RA) treatment on protein expression of CD36 and TGM2. Treatment conditions were 12-h incubation with 0.5 μM all-*trans*RA (tRA) followed by 8 h myelin exposure or either one of these treatments. (a, b) Effect of RA on protein expression of CD36 in Raw264.7 cells (a) and bone marrow–derived macrophages (BMDM) (b); (c, d) effect of RA on protein expression of TGM2 in Raw264.7 cells (c) and BMDM (d); for quantification the integrated density of CD36 and TGM2 IR bands was normalized to GAPDH and α-actinin, respectively ($n$ = 3-4; $^{*}p < .05$, $^{***}p < .001$ compared to control condition without myelin)

protein levels were increased by RA treatment, and blocking the activity of TGM2 reduced the RA-dependent increase of myelin endocytosis. Although we found macrophages to express a range of phagocytosis related receptors, including FcγR1, FcγR2b, FcγR3, TREM2, DAP12, CR3, MerTK, and CD36, none of these was significantly induced by RA treatment in the absence of myelin. The combination of RA and myelin exposure reduced the expression of M1 marker genes iNOS and IL-1β and increased expression of CD36 and ABC-A1, which are involved in lipid transport and metabolism.

In the CNS, cellular debris is cleared by macrophages, which originate from two sources. Under pathological conditions, resident microglia are activated, undergo a morphological change and become phagocytes. Secondly, in many pathologies, such as severe SCI, the blood brain barrier is disrupted allowing the massive influx of blood-derived macrophages. Both cell populations, which are morphologically indistinguishable, participate in the removal of myelin debris (Brück et al., 1995, Church et al., 2017, Neumann et al., 2009). Recent investigations indicate that astrocytes also contribute to the clearance of myelin (Wang et al., 2020). Unfortunately, after SCI the activity of these three cell populations is not sufficient to create a proregenerative environment. Myelin debris accumulates in the tissue and persists there for many months (Becerra et al., 1995), which

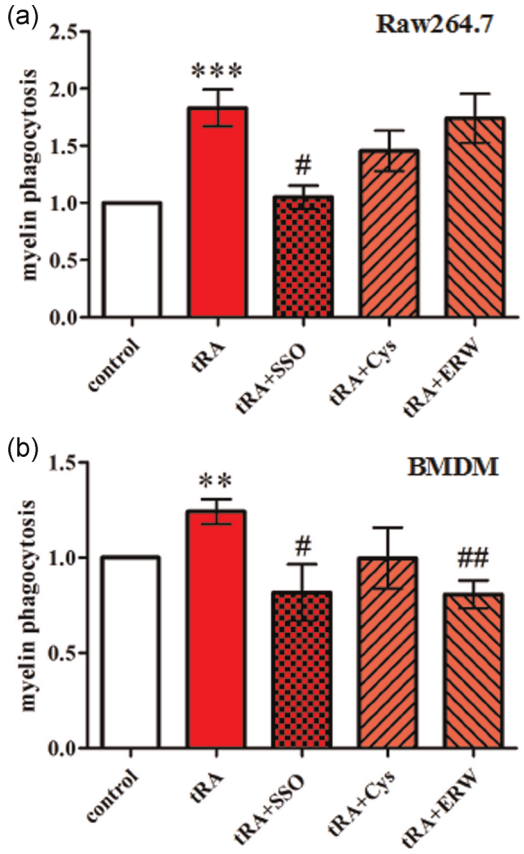


**FIGURE 8** Implication of CD36 and TGM2 in the effect of retinoic acid (RA) on myelin phagocytosis. To test the involvement of CD36 and TGM2, myelin endocytosis was measured with the pHrodo assay using 0.5 μM all-*trans*RA (tRA), combined with either 25 μM sulfo-*N*-succinimidyl oleate (SSO), 0.5 μM cystamine hydrochloride, or 50 μM ERW1041E. This was followed by 8 h myelin exposure. (a) Quantification of myelin phagocytosis in Raw264.7 cells showed a significant increase after RA treatment ($^{***}p < .001$), which was abolished in the presence of the CD36 inhibitor ($^{\#}p < .05$) and reduced, though not significantly when TGM2 activity was inhibitied ($n = 6$). (b) The same tendency was observed in bone marrow–derived macrophages, although the effect of RA ($^{**}p < .01$) was smaller (effect of inhibitors: $^{\#}p < .05$, $^{\#\#}p < .01$ in comparison with RA treatment only; $n = 4$). Data are normalized to the control condition without RA treatment

is in contrast to the situation after peripheral nerve lesions, where cellular debris is cleared efficiently, and axonal regeneration occurs. The present experiments suggest that the clearance of myelin by macrophages can be improved using RA, which at the same time reduces the inflammatory response. Increased synthesis of tRA and activation of RAR/RXR are among the endogenous responses to SCI (Mey et al., 2005; Schrage et al., 2006). Since the pharmacological activation of RAR is beneficial in animal models of SCI (Agudo et al., 2010; Gonçalves et al., 2015, 2018), ischemia (Cai et al., 2019) and neurodegenerative diseases (van Neerven et al., 2008), the present study points to an additional physiological target of RA treatment. It remains to be seen whether the modulation of phagocytosis is also an endogenous function of RA in vivo.

We investigated the effect of RA treatment on the expression of receptors that may mediate myelin endocytosis. Conceptually, phagocytosis mechanisms can be distinguished based on the criterion whether they are accompanied or not by inflammatory reactions of the phagocytes. Receptors that induce a proinflammatory response are those that recognize exogenous material such as bacterial pathogens (Neumann et al., 2009). These include toll-like receptors and antigen binding FcγR. Their activation triggers the release of inflammatory cytokines, prostaglandins, nitric oxide, and reactive oxygen species. Since high levels of these can be cytotoxic, an increase of this kind of phagocytosis is not desired from a therapeutic point of view. Given that RA has predominantly anti-inflammatory effects (Austenaa et al., 2009; Kampmann et al., 2008; van Neerven, Nemes, et al., 2010), it was not surprising to find that RA treatment of macrophages did not induce expression of these receptors in the presence of myelin. A second, noninflammatory process of phagocytosis, on the other hand, is considered to be beneficial. Receptors that recognize apoptotic cells respond to phosphatidylserine when it is exposed on the outer leaflet of the plasma membrane, thereby constituting an "eat-me"-signal. TREM-2, which acts as a sensor for lipid components, is a characteristic signaling molecule in this "silent" phagocytosis (Neumann et al., 2009). We did not find evidence that would implicate this mechanism in the effect of RA on myelin uptake.

Phagocytosis can also be categorized on whether the ingested material is opsonized, that is, tagged with antibodies or complements, or not (Flannagan et al., 2012). Opsonized particles activate the FcγR or the CR pathways. A key molecule of the complement pathway in the CNS is the CR3, also designated as $\alpha_M\beta_2$-integrin, CD11b/CD18 or macrophage-1 antigen. The CR3 binds to particles, including myelin, when they are marked with complement iC3b and thereby destined for phagocytosis. Clearance of nonopsonized myelin is regulated through receptors that are commonly referred to as pattern recognition receptors. These include carbohydrate receptors (lectins, e.g., galectin-3), lipoprotein binding scavenger receptor AI/II (SRAI/II), MerTK, and macrophage receptor with a collagenous structure (MARCO; Józefowski et al., 2005; Hendrickx et al., 2013). Binding of substrate to a phagocytosis receptor triggers engulfment by means of the contractile actin–myosin system of the cytoskeleton. In the process of internalization of IgG-opsonized particles, the activated FcγR cluster in the membrane, become phosphorylated and recruit intracellular adapter proteins, which initiate signaling cascades necessary for formation of the phagosome. Complement-mediated phagocytosis differs morphologically from the FcγR pathway and activates other signaling pathways, notably the GTPase Rho (Flannagan et al., 2012). We expected the gene expression of some of these receptors to be affected by RA treatment or the combination of myelin exposure and RA, but this was not the case.

However, when macrophages were pretreated with RA and then exposed to myelin, they showed increased gene expression of the receptor CD36. This transmembrane glycoprotein is a member of the class B scavenger receptor family that acts as a fatty acid translocase. CD36 is involved in the phagocytosis of apoptotic cells (Fadok et al., 1998). Recently, CD36 was shown to be required for the uptake of

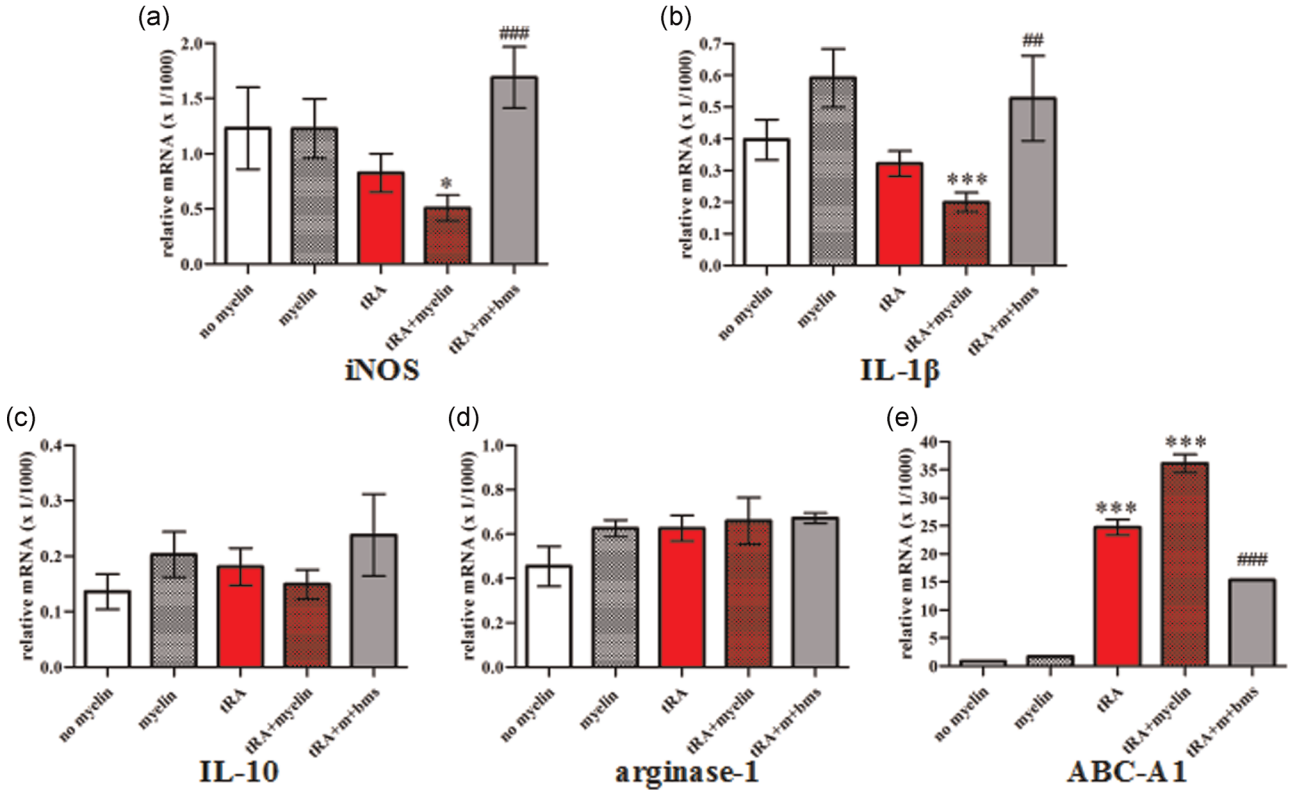


**FIGURE 9** Influence of myelin and retinoic acid (RA) on the inflammatory phenotype of Raw264.7 cells. Treatment conditions were 12-h incubation with 0.5 μM all-*trans*RA (tRA) followed by 8-h exposure to myelin. Together with RA and myelin we added 10 μM of the RARα/γ inhibitor BMS189453 (marked tRA + m + bms); messenger RNA was measured with quantitative real-time polymerase chain reaction and expressed relative to the control gene RPL4. (a) Expression of inducible nitric oxide synthase ($n = 4$; analysis of variance, $F = 2.9$, $df = 4$, $p < .05$); (b) of interleukin- 1β (IL-1β; $F = 5.6$, $df = 4$, $p < .01$); (c) IL-10 (n.s.), (d) arginase-1 (n.s.), and (e) ABC-A1 ($F = 684$, $df = 4$, $p < .0001$). Bars indicate means ± *SEM*, with post hoc Tukey tests $^{*}p < .05$, $^{***}p < .001$ versus myelin exposure; $^{\#\#}p < .01$, $^{\#\#\#}p < .001$ versus RA + myelin

myelin debris by microglia and macrophages (Grajchen et al., 2020). Inhibition of this receptor reduced the clearance of myelin debris by both types of phagocytes, promoting their inflammatory phenotype in vivo. When we blocked CD36 with SSO in the present experiments, the stimulating effect of RA was abolished. However, on the protein level no changes of CD36 were found, and in the absence of RA, SSO did not reduce myelin phagocytosis. Therefore, the involvement of CD36 in the effects reported here remains elusive. We speculate that RA-dependent changes of TGM2 may affect the intracellular localization of CD36.

We identified one link between RA signaling and the phagocytosis mechanism, which was the enzyme TGM2. In accordance with published results (C. Chen et al., 2019; Rébé et al., 2009; van Neerven, Regen, et al., 2010) tRA induced mRNA and protein expression of TGM2, and this was even stronger when macrophages were also exposed to myelin. The inhibition of TGM2 enzyme activity reduced the internalization of myelin. TGM2 might support the formation of the engulfing portals thereby increasing the efficiency of phagocytosis (Tóth et al., 2009). In TGM2-deficient macrophages the internalization of opsonized apoptotic thymocytes was significantly reduced (Szondy et al., 2003). Recently, TGM2 expression was also shown to contribute to myelin phagocytosis. TGM2-deficient macrophages, while not having a reduced uptake of myelin, showed increased accumulation of myelin compared to control cells (Sestito et al., 2020). The authors propose that TGM2 might be involved in the myelin degradation. Their work also provides an interesting link between this enzyme and the inflammatory state of macrophages because knockdown of TGM2 impaired the differentiation of monocyte-derived macrophages towards an anti-inflammatory phenotype (Sestito et al., 2020).

Does the phagocytosis of myelin trigger a pro- or anti-inflammatory phenotype? Myelin contains 70%–80% lipids, including a high content of saturated long-chain fatty acids, glycosphingolipids, and 40% cholesterol. Among the proteins, MBP, and proteolipid protein are most abundant in CNS myelin (Simons & Nave, 2016). When macrophages encounter these stimuli or accumulate lipids after endocytosis, they are induced to release proinflammatory cytokines and reactive oxygen species. In an animal model of SCI, the CR3-mediated uptake of myelin activated phosphatidylinositol-3-kinase/protein kinase B/nuclear factor-κB signaling and thereby induced a proinflammatory M1-like phenotype (Sun et al., 2010). However, cell culture studies have yielded conflicting data that implicate myelin also as an anti-inflammatory stimulus that induces an M2 phenotype, depending on additional environmental signals

(Kopper and Gensel, 2018). Since scavenger receptor and CR pathways can initiate alternative phenotypes (Józefowski et al., 2005), the cellular response may be determined by the receptor equipment of the cells when they are presented with myelin debris. For instance, prestimulation with interferon-γ modulated the response of microglia to myelin with a biphasic temporal pattern. It enhanced production of proinflammatory mediators during the first phase (≤6 h), followed by suppression during the second (6–24 h) phase (Liu et al., 2006). The cell culture experiments reported here demonstrate that myelin exposure alone did not change the phenotype of BMDM. In vivo, the effect of myelin processing on M1/M2 macrophage polarization remains controversial (Kopper and Gensel, 2018). Given the goal of improving the clearance of myelin debris after SCI, the challenge consists in achieving this without inducing a proinflammatory state of the phagocytes.

In models of multiple sclerosis, the uptake of myelin modified the physiology of macrophages via activation of MerTK, LXR, and PPARβ/δ signaling, suggesting an autoregulatory feedback of myelin clearance (Bogie et al., 2013, 2012). In contrast, myelin exposure did not affect the expression of MerTK in our BMDM and Raw264.7 cell cultures nor did the pharmacological activation of LXR or PPARβ/δ enhance myelin uptake. Different regulatory mechanisms may occur in demyelinating disorders and BMDM in vitro.

As mentioned in Section 1, RA reduces expression of inflammatory mediators (Dheen et al., 2005; Gross et al., 1993; Kampmann et al., 2008; van Neerven, Nemes, et al., 2010, van Neerven, Regen, et al., 2010), and this in macrophages is interpreted as a successful transition of M1–M2 phenotype (Vellozo et al., 2017). For this reason we expected that a stimulation of macrophage phagocytosis with retinoids would also induce them to develop a noninflammatory phenotype. Using key markers for M1/M2 phenotypes the present data corroborate the anti-inflammatory effect of RA and even show a synergistic effect in the presence of myelin. Expression of cytokine IL-10 and enzyme Arg-1, which are indicative of an M2 phenotype were not affected either by myelin or RA. Based on the potential to enhance myelin clearance while suppressing inflammation, clinical investigations into RA as a therapeutic agent in SCI patients are warranted.

## ACKNOWLEDGMENTS

Expert assistance was provided by the HNP core facilities of microscopy and cytometry. In particular, the authors thank Virginia Vila del Sol for evaluating DiO phagocytosis assays and José Ángel Rodríguez Alfaro and Javier Mazarío for help with confocal microscopy.

## CONFLICT OF INTERESTS

The authors declare that there are no conflict of interests.

## AUTHOR CONTRIBUTIONS

Jörg Mey and Lorenzo Romero-Ramírez designed and supervised the study and participated in data analysis. Siyu Wu performed the experiments and analyzed the data. Jörg Mey wrote the manuscript. All authors participated in proofreading.

## DATA AVAILABILITY STATEMENT

All relevant information is presented within the article. Additional data that support the findings of this study are available from the corresponding author upon reasonable request.

## ORCID

*Lorenzo Romero-Ramírez* http://orcid.org/0000-0002-8974-6698
*Jörg Mey* https://orcid.org/0000-0002-8919-3149

## REFERENCES

Agudo, M., Yip, P., Davies, M., Bradbury, E., Doherty, P., McMahon, S., Maden, M., & Corcoran, J. P. (2010). A retinoic acid receptor beta agonist (CD2019) overcomes inhibition of axonal outgrowth via phosphoinositide 3-kinase signalling in the injured adult spinal cord. *Neurobiology of Disease*, *37*, 147–155.

Allenby, G., Bocquel, M.-T., Saunders, M., Kazmer, S., Speck, J., Rosenberger, M., Lovey, A., Kastner, P., Grippo, J. F., Chambon, P., & Levin, A. A. (1993). Retinoic acid receptors and retinoid X receptors: Interactions with endogenous retinoic acids. *Proceedings of the National Academy of Sciences of the United States of America*, *90*, 30–34.

Austenaa, L. M., Carlsen, H. C., Hollung, K., Blomhoff, H. K., & Blomhoff, R. (2009). Retinoic acid dampens LPS-induced NF-kappaB activity: Results from human monoblasts and in vivo imaging of NF-kappaB reporter mice. *Journal of Nutritional Biochemistry*, *20*, 726–734.

Barton, W. A., Liu, B. P., Tzvetkova, D., Jeffrey, P. D., Fournier, A. E., Sah, D., Cate, R., Strittmatter, S. M., & Nikolov, D. B. (2003). Structure and axon outgrowth inhibitor binding of the Nogo-66 receptor and related proteins. *EMBO Journal*, *22*, 3291–3302.

Becerra, J. L., Puckett, W. R., Hiester, E. D., Quencer, R. M., Marcillo, A. E., & Post, M. J. (1995). MR-pathologic comparisons of Wallerian degeneration in spinal cord injury. *American Journal of Neuroradiology*, *16*, 125–133.

Bogie, J. F., Jorissen, W., Mailleux, J., Nijland, P. G., Zelcer, N., Vanmierlo, T., Van Horssen, J., Stinissen, P., Hellings, N., & Hendriks, J. J. (2013). Myelin alters the inflammatory phenotype of macrophages by activating PPARs. *Acta Neuropathologica Communications*, *1*, 43. https://doi.org/10.1186/2051-5960-1-43

Bogie, J. F., Timmermans, S., Huynh-Thu, V. A., Irrthum, A., Smeets, H. J., Gustafsson, J. A., Steffensen, K. R., Mulder, M., Stinissen, P., Hellings, N., & Hendriks, J. J. (2012). Myelin-derived lipids modulate macrophage activity by liver X receptor activation. *PLOS One*, *7*, e44998. https://doi.org/10.1371/journal.pone.0044998

Brück, W., Porada, P., Poser, S., Rieckmann, P., Hanefeld, F., Kretzschmar, H. A., & Lassmann, H. (1995). Monocyte/macrophage differentiation in early multiple sclerosis lesions. *Annals of Neurology*, *38*, 788–796.

Buss, A., Pech, K., Merkler, D., Kakulas, B. A., Martin, D., Schoenen, J., Noth, J., Schwab, M. E., & Brook, G. A. (2005). Sequential loss of myelin proteins during Wallerian degeneration in the human spinal cord. *Brain*, *128*, 356–364.

Cai, W., Wang, J., Hu, M., Chen, X., Lu, Z., Bellanti, J. A., & Zheng, S. G. (2019). All trans-retinoic acid protects against acute ischemic stroke by modulating neutrophil functions through STAT1 signaling. *Journal of Neuroinflammation*, *16*, 175. https://doi.org/10.1186/s12974-019-1557-6

Caprariello, A. V., Rogers, J. A., Morgan, M. L., Hoghooghi, V., Plemel, J. R., Koebel, A., Tsutsui, S., Dunn, J. F., Kotra, L. P., Ousman, S. S., Wee Yong, V., & Stys, P. S. (2018). Biochemically altered myelin triggers autoimmune demyelination. *Proceedings of the National Academy of Sciences of United States of America*, *115*, 5528–5533.

Chen, M. S., Huber, A. B., van der Haar, M. E., Frank, M., Schnell, L., Spillmann, A. A., Christ, F., & Schwab, M. E. (2000). Nogo-A is a myelin-

associated neurite outgrowth inhibitor and an antigen for monoclonal antibody IN-1. *Nature*, *403*, 434–439.

Chen, C., Perry, T. L., Chitko-McKown, C. G., Smith, A. D., Cheung, L., Beshah, E., Urban, J. F., Jr., & Dawson, H. D. (2019). The regulatory actions of retinoic acid on M2 polarization of porcine macrophages. *Devlopmental and Comparative Immunology 98*, 20–33.

Chrobok, N. L., Bol, J. G. J. M., Jongenelen, C. A., Brevé, J. J. P., El Alaoui, S., Wilhelmus, M. M. M., Drukarch, B., & van Dam, A.-M. (2018). Characterization of Transglutaminase 2 activity inhibitors in monocytes in vitro and their effect on a mouse model for multiple sclerosis. *PLOS One*, *13*(4), e019643. https://doi.org/10.1371/journal.pone.0196433

Church, J. S., Milich, L. M., Lerch, J. K., Popovich, P. G., & McTigue, D. M. (2017). E6020, a synthetic TLR4 agonist, accelerates myelin debris clearance, Schwann cell infiltration, and remyelination in the rat spinal cord. *Glia*, *65*, 883–899.

Dheen, S. T., Jun, Y., Yan, Z., Tay, S. S., & Ling, E. A. (2005). Retinoic acid inhibits expression of TNF-alpha and iNOS in activated rat microglia. *Glia*, *50*, 21–31.

Ek, C. J., Habgood, M. D., Dennis, R., Dziegielewska, K. M., Mallard, C., Wheaton, B., & Saunders, N. R. (2012). Pathological changes in the white matter after spinal contusion injury in the rat. *PLOS One*, *7*, e43484. https://doi.org/10.1371/journal.pone.0043484

Eligini, S., Fiorelli, S., Tremoli, E., & Colli, S. (2016). Inhibition of transglutaminase 2 reduces efferocytosis in human macrophages: Role of CD14 and SR-AI receptors. *Nutrition, Metabolism, and Cardiovascular Diseases*, *26*, 922–930.

Fadok, V., Warner, M. L., Bratton, D. L., & Henson, P. M. (1998). CD36 is required for phagocytosis of apoptotic cells by human macrophages that use either a phosphatidylserine receptor or the vitronectin receptor (alpha v beta 3). *Journal of Immunology*, *161*, 6250–6279.

Flannagan, R. S., Jaumouillé, V., & Grinstein, S. (2012). The cell biology of phagocytosis. *Annual Review of Pathology: Mechanisms of Disease*, *7*, 61–98.

Fournier, A. E., Gould, G. C., Liu, B. P., & Strittmatter, S. M. (2002). Truncated soluble Nogo receptor binds Nogo-66 and blocks inhibition of axon growth by myelin. *Journal of Neuroscience*, *22*, 8876–8883.

Gonçalves, M. B., Malmqvist, T., Clarke, E., Hubens, C. J., Grist, J., Hobbs, C., Trigo, X. D., Risling, M., Damberg, M. A. P., Carlstedt, T. P., & Corcoran, J. P. Y. (2015). Neuronal RAR signaling modulates PTEN activity directly in neurons and via exosome transfer in astrocytes to prevent glial scar formation and induce spinal cord regeneration. *Journal of Neuroscience*, *25*, 15731–15745.

Gonçalves, M. B., Wu, Y., Trigo, D., Clarke, E., Malmqvist, T., Grist, J., Hobbs, C., Carlstedt, T. P., & Corcoran, J. P. T. (2018). Retinoic acid synthesis by NG2 expressing cells promotes a permissive environment for axonal outgrowth. *Neurobiology of Disease*, *111*, 70–79.

Grajchen, E., Hendriks, J. J. A., & Bogie, J. F. J. (2018). The physiology of foamy phagocytes in multiple sclerosis. *Acta Neuropathologica Communications*, *6*, 124. https://doi.org/10.1186/s40478-018-0628-8

Grajchen, E., Wouters, E., van de Haterd, B., Haidar, M., Hardonnière, K., Dierckx, T., Van Broeckhoven, J., Erens, C., Hendrix, S., Kerdine-Römer, S., & Hendriks, J. J. A. (2020). CD36-mediated uptake of myelin debris by macrophages and microglia reduces neuroinflammation. *Journal of Neuroinfllamation*, *17*, 224. https://doi.org/10.1186/s12974-020-01899-x

Greenhalgh, A. D., & David, S. (2014). Differences in the phagocytic response of microglia and peripheral macrophages after spinal cord injury and its effects on cell death. *Journal of Neuroscience*, *34*, 6316–6322. https://doi.org/10.1523/JNEUROSCI.4912-13.2014

Gross, V., Villiger, P. M., Zhang, B., & Lotz, M. (1993). Retinoic acid inhibits interleukin-1-induced cytokine synthesis in human monocytes. *Journal of Leukocyte Biology*, *54*, 125–132.

Hendrickx, D. A., Koning, N., Schuurman, K. G., van Strien, M. E., van Eden, C. G., Hamann, J., & Huitinga, I. (2013). Selective upregulation of scavenger receptors in and around demyelinating areas in multiple sclerosis. *Journal of Neuropathology and Experimental Neurology*, *72*, 106–118. https://doi.org/10.1097/NEN.0b013e31827fd9e8

Huang, J. K., Jarjour, A. A., Oumesmar, B. N., Kerninon, C., Williams, A., Krezel, W., Kagechika, H., Bauer, J., Zhao, C., Baron-Van Evercooren, A., Chambon, P., ffrench-Constant, C., & Franklin, R. J. M. (2011). Retinoid X receptor gamma signaling accelerates CNS myelination. *Nature Neuroscience*, *14*, 45–53.

Józefowski, S., Arredouani, M., Sulahian, T., & Kobzik, L. (2005). Disparate regulation and function of the class A scavenger receptors SR-AI/II and MARCO. *Journal of Immunology*, *175*, 8032–8041. https://doi.org/10.4049/jimmunol.175.12.8032

Kampmann, E., Johann, S., van Neerven, S., Beyer, C., & Mey, J. (2008). Anti-inflammatory effect of retinoic acid on prostaglandin synthesis in cultured cortical astrocytes. *Journal of Neurochemistry*, *106*, 320–332.

Kopper, T. J., & Gensel, J. C. (2018). Myelin as an inflammatory mediator: Myelin interactions with complement, macrophages, and microglia in spinal cord injury. *Journal of Neuroscience Research*, *96*, 969–977.

Kotter, M. R., Li, W.-W., Zhao, C., & Franklin, R. J. M. (2006). Myelin impairs CNS remyelination by inhibiting oligodendrocyte precursor cell differentiation. *Journal of Neuroscience*, *26*, 328–332.

Larange, A., & Cheroutre, H. (2016). Retinoic acid and retinoic acid receptors as pleiotropic modulators of the immune system. *Annual Review of Immunology*, *34*, 369–394.

Liu, Y., Hao, W., Letiembre, M., Walter, S., Kulanga, M., Neumann, H., & Fassbender, K. (2006). Suppression of microglial inflammatory activity by myelin phagocytosis: Role of p47-PHOX-mediated generation of reactive oxygen species. *Journal of Neuroscience*, *26*, 12904–12913.

McKerracher, L., David, S., Jackson, D. L., Kottis, V., Dunn, R. J., & Braun, P. E. (1994). Identification of myelin-associated glycoprotein as a major myelin-derived inhibitor of neurite growth. *Neuron*, *13*, 805–811.

Mey, J. (2017). RAR/RXR-mediated signaling. In S. Mandal (Ed.), *Gene regulation, epigenetics, and hormone signaling* (pp. 457–512). Wiley-VCH.

Mey, J., Morassutti, D. J., Brook, G., Liu, R.-H., Zhang, Y.-P., Koopmans, G., & McCaffery, P. (2005). Retinoic acid synthesis by a population of NG-positive cells in the injured spinal cord. *European Journal of Neuroscience*, *21*, 1555–1568.

Mey, J., Schrage, K., Weßels, I., & Vollpracht-Crijns, I. (2007). Effects of inflammatory cytokines IL-1β, IL-6 and TNFα on the intracellular localization of retinoid receptors in Schwann cells. *Glia*, *55*, 152–164.

Morizawa, Y. M., Hirayama, Y., Ohno, N., Shibata, S., Shigetomi, E., Sui, Y., Nabekura, J., Sato, K., Okajima, F., Takebayashi, H., Okano, H., & Koizumi, S. (2017). Reactive astrocytes function as phagocytes after brain ischemia via ABCA1-mediated pathway. *Nature Communications*, *8*(1), 28. https://doi.org/10.1038/s41467-017-00037-1

Nadella, V., Wang, Z., Johnson, T. S., Griffin, M., & Devitt, A. (2015). Transglutaminase 2 interacts with syndecan-4 and CD44 at the surface of human macrophages to promote removal of apoptotic cells. *Biochimica et Biophysica Acta/General Subjects*, *1853*, 201–212.

van Neerven, S., Kampmann, E., & Mey, J. (2008). RAR/RXR and PPAR/RXR signaling in neurological and psychiatric diseases. *Progress in Neurobiology 85*, 433–451.

van Neerven, S., Nemes, A., Imholz, P., Regen, T., Denecke, B., Johann, S., Beyer, C., Hanisch, U.-K., & Mey, J. (2010). Inflammatory cytokine release of astrocytes in vitro is reduced by all-*trans* retinoic acid. *Journal of Neuroimmunology*, *229*, 169–179.

van Neerven, S., Regen, T., Wolf, D., Nemes, A., Johann, S., Beyer, C., Hanisch, U.-K., & Mey, J. (2010). Inflammatory chemokine release of astrocytes in vitro is reduced by all-*trans* retinoic acid. *Journal of Neurochemistry*, *114*, 1511–1526.

Neumann, H., Kotter, M. R., & Franklin, R. J. M. (2009). Debris clearance by microglia: An essential link between degeneration and regeneration. *Brain*, *132*, 288–295. https://doi.org/10.1093/brain/awn109

Rébé, C., Raveneau, M., Chevriaux, A., Lakomy, D., Sberna, A.-L., Costa, A., Bessède, G., Athias, A., Steinmetz, E., Lobaccaro, J. M. A., Alves, G., Menicacci, A., Vachenc, S., Solary, E., Gambert, P., & Masson, D. (2009). Induction of transglutaminase 2 by a liver X receptor/retinoic acid receptor pathway increases the clearance of apoptotic cells by human macrophages. *Circulation Research*, *105*, 393–401.

Röszer, T. (2017). Transcriptional control of apoptotic cell clearance by macrophage nuclear receptors. *Apoptosis*, *22*, 284–294.

Schnell, L., & Schwab, M. E. (1990). Axonal regeneration in the rat spinal cord produced by an antibody against myelin-associated neurite growth inhibitors. *Nature*, *343*, 269–272.

Schrage, K., Koopmans, G., Joosten, E. A., & Mey, J. (2006). Macrophages and neurons are targets of retinoic acid signaling after spinal cord contusion injury. *European Journal of Neuroscience*, *23*, 285–295.

Sestito, C., Brevé, J. J. P., Bol, J. G. J. M., Wilhelmus, M. M. M., Drukarch, B., & van Dam, A.-M. (2020). Tissue transglutaminase contributes to myelin phagocytosis in interleukin-4-treated human monocyte-derived macrophages. *Cytokine*, *128*, 155024. https://doi.org/10.1016/j.cyto.2020.155024

Simons, M., & Nave, K.-A. (2016). Oligodendrocytes: Myelination and axonal support, *Cold Spring Harbor Perspectives in Biology*. Cold Spring Harbor Laboratory Press. https://doi.org/10.1101/cshperspect.a020479

Sun, X., Wang, X., Chen, T., Li, T., Cao, K., Lu, A., Chen, Y., Sun, D., Luo, J., Fan, J., Young, W., & Ren, Y. (2010). Myelin activates FAK/Akt/NF-kappaB pathways and provokes CR3-dependent inflammatory response in murine system. *PLOS One*, *5*, e9380. https://doi.org/10.1371/journal.pone.0009380

Szondy, Z., Saran, Z., Molnár, P., Németh, T., Piacentini, M., Mastroberardino, P. G., Falasca, L., Aeschlimann, D., Kovács, J., Kiss, I., Szegezdi, É., Lakos, G., Rajnavölgyi, É., Birckbichler, P. J., Melino, G., & Fésüs, L. (2003). Transglutaminase 2−/− mice reveal a phagocytosis-associated crosstalk between macrophages and apoptotic cells. *Proceedings of the National Academy of Sciences of United States of America*, *100*, 7812–7817.

Tóth, B., Garabuczi, É., Sarang, Z., Vereb, G., Vámosi, G., Aeschlimann, D., Blaskó, B., Bécsi, B., Erdõdi, F., Lacy-Hulbert, A., Zhang, A., Falasca, L., Birge, R. B., Balajthy, Z., Melino, G., Fésüs, L., & Szondy, Z. (2009). Transglutaminase 2 is needed for the formation of an efficient phagocyte portal in macrophages engulfing apoptotic cells. *Journal of Immunology*, *182*, 2084–2092.

Vellozo, N. S., Pereira-Marques, S., Cabral-Piccin, M. P., Filardy, A. A., Ribeiro-Gomes, F., Rigoni, T. S., DosReis, G. A., & Lopes, M. F. A. (2017). All-*rrans* retinoic acid promotes an M1- to M2-phenotype shift and inhibits macrophage-mediated immunity to *Leishmania major*. *Frontiers in Immunology*, *8*, 1580. https://doi.org/10.3389/fimmu.2017.01560

Wang, S., Deng, J., Fu, H., Guo, Z., Zhang, L., & Tang, P. (2020). Astrocytes directly clear myelin debris through endocytosis pathways and followed by excessive gliosis after spinal cord injury. *Biochemical and Biophysical Research Communications*, *525*, 20–26.

Zhelyaznik, N., Schrage, K., McCaffery, P., & Mey, J. (2003). Activation of retinoic acid signaling after sciatic nerve injury: upregulation of cellular retinoid binding proteins. *European Journal of Neuroscience*, *18*, 1033–1040.

Zhou, Q., Xiang, H., Li, A., Lin, W., Huang, Z., Guo, J., Wang, P., Chi, Y., Xiang, K., Xu, Y., Zhou, L., So, K. F., Chen, X., Sun, X., & Ren, Y. (2019). Activating adiponectin signaling with exogenous AdipoRon reduces myelin lipid accumulation and suppresses macrophage recruitment after spinal cord injury. *Journal of Neurotrauma*, *36*, 903–918.

## SUPPORTING INFORMATION

Additional supporting information may be found online in the Supporting Information section.

**How to cite this article:** Wu S, Romero-Ramírez L, Mey J. Retinoic acid increases phagocytosis of myelin by macrophages. *J Cell Physiol*. 2021;236:3929–3945. https://doi.org/10.1002/jcp.30137